Lhx2$^{-/-}$ mice develop liver fibrosis

Ewa Wandzioch*, Åsa Kolterud*, Maria Jacobsson*, Scott L. Friedman†, and Leif Carlsson*‡

*Umeå Center for Molecular Medicine, Umeå University, 901 87 Umeå, Sweden; and †Division of Liver Diseases, Mount Sinai School of Medicine, New York, NY 10029-6574

Edited by Kathryn V. Anderson, Sloan–Kettering Institute, New York, NY, and approved October 12, 2004 (received for review June 30, 2004)

Liver fibrosis is a wound-healing response to chronic injury of any type and is characterized by a progressive increase in deposition of extracellular matrix (ECM) proteins, the major source of which are activated hepatic stellate cells (HSCs). Because the *LIM* homeobox gene *Lhx2* is expressed in HSCs and liver development in *Lhx2*$^{-/-}$ mice is disrupted, we analyzed liver development in *Lhx2*$^{-/-}$ embryos in detail. *Lhx2*$^{-/-}$ embryos contain numerous activated HSCs and display a progressively increased deposition of the ECM proteins associated with liver fibrosis, suggesting that Lhx2 inhibits HSC activation. Transfection of Lhx2 cDNA into a human HSC line down-regulates expression of genes characteristic of activated HSCs. Moreover, the *Lhx2*$^{-/-}$ liver display a disrupted cellular organization and an altered gene expression pattern of the intrahepatic endodermal cells, and the increased deposition of ECM proteins precedes these abnormalities. Collectively these results show that Lhx2 negatively regulates HSC activation, and its inactivation in developing HSCs appears therefore to mimic the signals that are triggered by the wound-healing response to chronic liver injury. This study establishes a spontaneous and reproducible animal model for hepatic fibrosis and reveals that Lhx2 expression in HSCs is important for proper cellular organization and differentiation of the liver.

hepatic stellate cells | cirrhosis | liver regeneration

Liver fibrosis and its end stage cirrhosis represent an enormous worldwide health-care problem. The common causes of liver fibrosis are different chronic injuries inflicted on the liver, such as alcohol abuse, viral hepatitis, bile-duct obstruction, immune mediated damage, and a group of developmental abnormalities collectively referred to as congenital hepatic fibrosis (1–3). The development of fibrosis is the result of the sustained wound-healing process that occurs in the liver in response to the different chronic injuries (1, 4). All forms of fibrosis and cirrhosis, independent of the underlying etiology, have several common features, such as excessive and disorderly deposition of extracellular matrix (ECM) proteins and distorted hepatic architecture, that eventually can lead to impairment of liver function (5–7).

Several lines of evidence support the hypothesis that the hepatic stellate cell (HSC) (also known as lipocyte, fat-storing cell, or Ito cell) is the central mediator of the fibrogenic process. In a normal liver, HSCs store retinoids and are localized in the subendothelial space of Disse that separates the hepatocytes from the sinusoidal endothelium (8, 9). In the injured areas of the liver, HSCs become activated and undergo transformation into myofibroblast-like cells. The activated HSCs start to proliferate and are the main source of the ECM proteins that are known to accumulate in fibrotic livers (10–13). The external stimuli that trigger activation of HSCs have been studied extensively both in patient material and animal models, but the genes mediating the response in HSCs are largely unknown (2).

We have recently shown that the LIM homeobox gene *Lhx2* is expressed in HSCs in the adult liver (14). *Lhx2*$^{-/-}$ embryos develop liver hypoplasia and die at approximately embryonic day 16 (E16) of anemia caused by an uncharacterized defect in nonhematopoietic mesenchymal cells (14, 15). Because the fibrogenic process in liver fibrosis and cirrhosis is caused by phenotypically altered HSCs (1, 4, 11, 16), we investigated liver development in *Lhx2*$^{-/-}$ embryos in detail. Interestingly, the *Lhx2*$^{-/-}$ mouse embryos develop a spontaneous and progressive hepatic fibrosis displaying many of the characteristics ascribed to the pathogenic process occurring in patient material and in animal models of liver fibrosis.

Methods

Mice and Embryos. Generation of *Lhx2*$^{-/-}$ mice has been reported (15), and they were maintained and genotyped as described (14, 17). All experiments involving animals in this study have been approved by the ethical committee at Umeå University.

Immunohistochemistry, Antibodies, Histochemistry, and *in Situ* Hybridization. Two to six embryos from independent litters were analyzed in each staining. Collected tissues were fixed with 4% paraformaldehyde and embedded subsequently in either paraffin or OCT compound (Sakura, Zoeterwoude, The Netherlands). Paraffin-embedded sections were processed for hematoxylin–eosin staining or Gordon and Sweet's method for silver staining of reticulin fibers according to standard procedures. Immunostaining was carried out as described (18) by using the following primary antibodies: biotinylated rabbit anti-albumin, rat anti-E-cadherin, rabbit anti-α-fetoprotein (AFP), rabbit anti-desmin, mouse anti-desmin, rabbit anti-collagen IV, rabbit anti-laminin, rabbit anti-human cytokeratin, rat anti-PECAM-1, mouse Cy3-conjugated anti-α-smooth muscle actin (ASMA), and mouse anti-fibronectin. The following secondary antibodies were used for immunofluorescence: Cy3 anti-rabbit IgG, Alexa Fluor 488 goat anti-mouse IgG1, and donkey anti-rat IgG. *Dolichos biflorus* agglutinin conjugated to biotin was used. The albumin antibody and *D. biflorus* agglutinin was detected by using the avidin–biotin method and 3,3′-diaminobenzidine tetrachloride as a chromogen. The sections were routinely counterstained with 4′,6-diamidino-2-phenylindole for visualization of cell nuclei. Sources and catalog numbers of all of the antibodies and reagents that were used are described in *Supporting Methods*, which is published as supporting information on the PNAS web site. Antisense Lhx2 probe was prepared as described (14). *In situ* hybridization was carried out by using standard hybridization techniques with the modifications described in *Supporting Methods*. Confocal microscopy analyses were carried out as described (14). Quantification of desmin-positive cells is described in *Supporting Methods*.

RNA Preparation and Real-Time PCR Analyses. Total RNA was extracted from a pool of two to three livers from WT and mutant animals by the NucleoSpin purification kit (BD Biosciences). cDNA was synthesized by using the First Strand cDNA synthesis kit (Amersham Biosciences). Real-time PCR analyses were carried out in triplicates on three independent cDNA prepara-

This paper was submitted directly (Track II) to the PNAS office.

Freely available online through the PNAS open access option.

Abbreviations: AFP, α-fetoprotein; ASMA, α-smooth muscle actin; ECM, extracellular matrix; E*n*, embryonic day *n*; HSC, hepatic stellate cell; MMP, matrix metalloproteinase; TIMP, tissue inhibitor of metalloproteinases.

‡To whom correspondence should be addressed. E-mail: leif.carlsson@ucmm.umu.se.

tions from WT and mutant livers. A detailed description of the real-time PCR procedure and the primers that we used is given in *Supporting Methods*.

Transfection of LX-2 Cell Lines. Cells were seeded at 10^6 cells per dish in 10-cm culture dishes at 24 h before transfection. Cells were transfected by using 5 or 10 μg of mouse Lhx2 expression plasmid or empty vector (pcDNA3.1, Invitrogen) as control in 15 μl of Fugene reagent according to the manufacturer's recommendations. Cells were collected 24 h after transfection, total RNA was isolated by using RNeasy kit (Invitrogen) and a reverse transcription, and real-time PCR analyses were performed. No difference in viability between the cells transfected with Lhx2 plasmid or empty vector was observed. Five independent transfections were carried out with similar results.

Results

Increased Expression and Deposition of ECM Proteins in *Lhx2*$^{-/-}$ Fetal Livers. We initially compared fetal livers from *Lhx2*$^{-/-}$ and WT embryos at E14.5, at which time the liver is well developed and phenotypic differences between WT and mutant livers are easily discerned. In addition to the reduced size, the livers from mutant embryos contained fibrous-like tissue (Fig. 1*B*) not observed in WT livers (Fig. 1*A*), suggesting an ongoing fibrogenic process. The hallmark of fibrosis is increased deposition of various ECM proteins, such as the interstitial collagens type I and III, the glycoprotein fibronectin, and the basement membrane components collagen type IV and laminin (5, 6, 19). Therefore, we compared the ECM content in mutant livers with that of WT livers at the levels of protein deposition and gene expression. Abundant type III collagen deposits detected as reticulin fibers were found in the mutant livers (Fig. 1*D*), whereas sparse reticulin fibers were present in the perisinusoidal spaces in WT livers (Fig. 1*C*). The fibrosis is progressive because E12.5 mutant livers contained slightly increased levels of reticulin fibers (Fig. 1*F*) compared with WT livers (Fig. 1*E*), but the collagen III deposits in E12.5 mutant livers were not as prominent as in E14.5 mutant livers (compare Fig. 1 *D* and *F*). Also, deposition of the other ECM proteins known to accumulate during hepatic fibrosis (like collagen type IV, laminin, and fibronectin) was increased in the *Lhx2*$^{-/-}$ livers (Fig. 1 *H*, *J*, and *L*) as compared with WT livers (Fig. 1 *G*, *I*, and *K*). Gene-expression analysis using real-time PCR showed a 9-fold increase in expression levels of collagen type I [collagen 1α(I)] and a 2.5-fold increase in expression of prolyl-4-hydroxylase (which is a critical enzyme for the posttranslational modifications causing increased stability of the collagen triple helix) in mutant livers as compared with WT livers (Fig. 1*M*). Thus, loss of Lhx2 expression leads to increased expression and a progressive accumulation of the ECM proteins associated with liver fibrosis, confirming an ongoing fibrogenic process in *Lhx2*$^{-/-}$ fetal livers.

Increased Proportion of HSCs with an Activated Phenotype in *Lhx2*$^{-/-}$ Fetal Liver. The HSC play a central role in the pathogenesis of liver fibrosis. We have shown (14) that Lhx2 is expressed in HSCs in the adult liver. Here, we show that Lhx2 is coexpressed with the HSC-specific marker desmin (20) (Fig. 2 *A–C*), confirming that Lhx2 is expressed in HSCs also in fetal liver. The proportion of desmin-positive cells was increased dramatically in mutant livers as compared with WT livers (Fig. 2 *D–F*), which is in agreement with the increase in number of HSCs that occurs during progressive hepatic fibrosis (1, 2). During the fibrogenic process, the HSCs become activated and acquire a phenotype resembling myofibroblast-like cells by expressing ASMA, in addition to desmin (21, 22). Consistent with this data, many of the desmin-positive cells also coexpressed ASMA in the mutant livers (Fig. 2 *J–L*), whereas this pattern was rarely detected in WT livers (Fig. 2 *G–I*), suggesting that at least a subpopulation of the HSCs in mutant livers acquired the phenotype of activated HSCs. Thus, the increased proportion of activated HSCs, together with the elevated deposition of ECM proteins in the mutant liver, suggests that loss of *Lhx2* expression in developing HSCs initiates pathological events similar to those observed in hepatic fibrosis.

Increased Expression of Genes Implicated in the Early Phase of HSC Activation in *Lhx2*$^{-/-}$ Fetal Liver. HSC activation is accompanied by changes in matrix protease activity, which leads to aberrant remodeling of the hepatic ECM proteins, and up-regulation of polypeptide growth-factor expression. Both of these alterations stimulate HSC activation in a direct and indirect manner (1, 23). Activated HSCs are a key source of matrix metalloproteinase (MMP)-2 and MMP-3, both of which degrade normal perisinusoidal liver matrix (23). Accelerated degradation of basement membrane components increases ECM protein synthesis and deposition of interstitial collagens, which in turn further activates HSCs in a positive feedback loop (1, 24). Activated HSCs can also favor accumulation of interstitial collagens by up-regulating tissue inhibitors of metalloproteinases (TIMPs) that inhibit the activity of MMP-13, which is an interstitial collagenase (23). Up-regulation of TIMPs may also lead to increased resistance to apoptosis of HSCs (25), which might contribute to the accumulation of HSCs in the fibrotic liver. To assess the matrix protease activity and growth-factor expression of cells in *Lhx2*$^{-/-}$ and WT livers, we compared the expression levels of various fibrosis-associated MMPs, TIMPs, and growth factors by real-time RT-PCR analysis (Fig. 3*A*). mRNA levels for TIMP1 and TIMP2 in the *Lhx2*$^{-/-}$ livers were up-regulated two and four times, respectively. MMP-2 and MMP-3 were up-regulated 3- and 2-fold in the mutant liver, respectively, whereas expression level of MMP-13 was unchanged, potentially contributing to the accumulation of interstitial collagens. Furthermore, platelet-derived growth factor, which is a potent mitogen for HSCs during early stages of HSC activation, showed a 4-fold up-regulation in mutant liver, whereas cytokines (such as transforming growth factor type β1 and tumor necrosis factor α) suggested to be involved in a later stage (the so-called perpetuation) of HSCs activation (1, 26) were unchanged. These data show that *Lhx2*$^{-/-}$ liver also develops many molecular changes that are typical for the early stage of HSC activation and liver fibrosis (1, 2, 23).

Lhx2 Expression in a Human Stellate Cell Line Down-Regulates Activation-Specific Genes. The phenotype observed in the *Lhx2*$^{-/-}$ fetal liver suggests that Lhx2 inhibits and/or suppresses activation of HSCs. To test this hypothesis, we transfected Lhx2 cDNA into the human HSC line LX-2 (which is a cell line showing the key features of HSCs; ref. 27) and measured the effect on expression levels of two genes associated with activated HSCs [ASMA and collagen 1α(I)]. These genes are reliable markers for activated HSCs, and were also consistently and significantly up-regulated in the *Lhx2*$^{-/-}$ livers as compared with WT livers (see Fig. 1*M*, compare Fig. 2 *H* with *K*, and data not shown). Cells transfected with Lhx2 revealed a 62% and 41% down-regulation of expression of ASMA and collagen 1α(I), respectively, as compared with cells transfected with empty vector (Fig. 3*B*). Thus, Lhx2 expression in a human HSC line lead to down-regulated expression of at least a subset of genes associated with activated HSCs.

Distorted Cellular Organization of the *Lhx2*$^{-/-}$ Fetal Liver. The three-dimensional structure of the liver is usually disrupted during the progression of fibrosis and cirrhosis (1). Therefore, the increased proportion of ECM proteins in *Lhx2*$^{-/-}$ livers might also interfere with the organization of the fetal liver. To address this issue, we analyzed the ECM protein production and the cellular organization of the mutant liver at different embry-

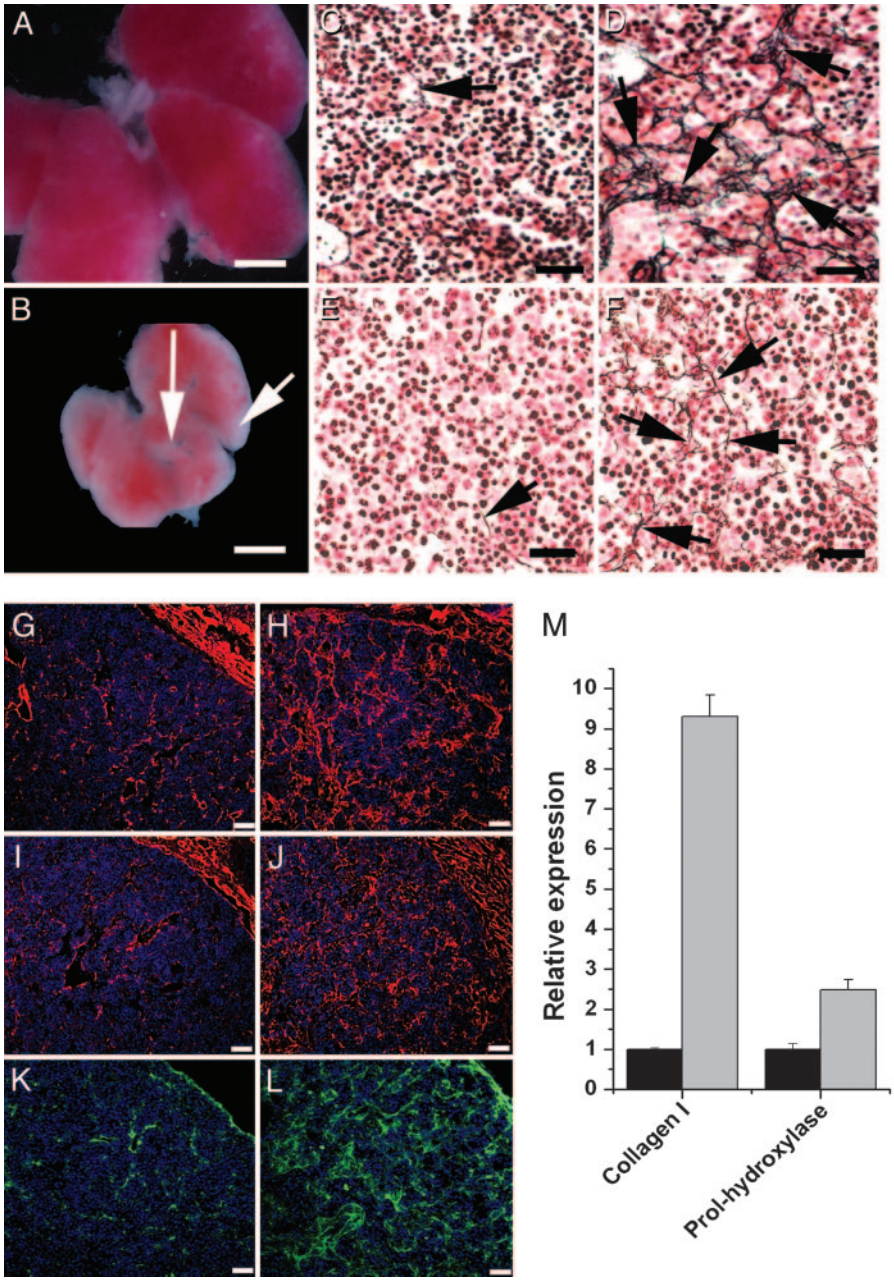

Fig. 1. Elevated deposition of ECM proteins and increased expression of ECM-associated genes in *Lhx2*$^{-/-}$ fetal livers. Fetal livers dissected from E14.5 WT (*A*) and *Lhx2*$^{-/-}$ (*B*) embryos showing fibrous-like tissue on the liver surface and between the liver lobes in the mutant (arrows). Histological sections of E14.5 WT (*C*, *G*, *I*, and *K*) and *Lhx2*$^{-/-}$ (*D*, *H*, *J*, and *L*) fetal livers, and of E12.5 WT (*E*) and *Lhx2*$^{-/-}$ (*F*) fetal livers. Sections treated with Gordon and Sweet's method for silver staining of reticulin fibers to visualize collagen type III fibers (arrows in *C–F*). Sections immunostained with anti-collagen IV (*G* and *H*, red), anti-laminin (*I* and *J*, red) and anti-fibronectin (*K* and *L*, green) antibodies. (*M*) Real-time PCR analyses comparing relative gene expression levels of collagen 1α(I) (Collagen I) and prolyl-4-hydroxylase (Prol-hydroxylase) in E14.5 WT (black bars) and *Lhx2*$^{-/-}$ (gray bars) livers. The data are presented as the mean value from one experiment done in triplicate. Similar results were obtained from two additional experiments performed on two other independently prepared cDNAs (data not shown). $P < 0.0001$ for collagen I, and $P < 0.005$ for prolhydroxylase. Error bars indicate standard deviation. (Scale bars indicate 1,000 μm in *A* and *B*, 30 μm in *C–F*, and 50 μm in *G–L*.)

onic stages. We observed an increased deposition of collagen IV in the mutant liver already at E11.5 (Fig. 4 *A* and *B*), with no obvious difference in the morphology or distribution of endodermal cells between mutant and WT livers (Fig. 4 *C* and *D*). In contrast, sections of the livers derived from E14.5 embryos revealed that the intrahepatic endoderm of the mutant livers was severely disorganized as compared with WT livers (Fig. 4 *E* and *F*) because the endodermal cells in mutant livers formed ductular structures that were not present in WT livers (Fig. 4*G*, see also Fig. 2*E*). However, the defect was specific for the intrahepatic endoderm because no obvious difference in the organization of the extrahepatic biliary epithelium was observed between WT and mutant embryos (Fig. 4 *J* and *K*). Fibrous tissue was easily discerned in mutant livers in the region of hilum (compare Fig. 4 *I* and *H*), around large vessels (compare Fig. 4 *M* and *L*), and throughout the liver as fibrous septa (Fig. 4*G*). A proper organization of the sinusoidal system in the liver is important for liver function (9). Although a normal sinusoidal network was

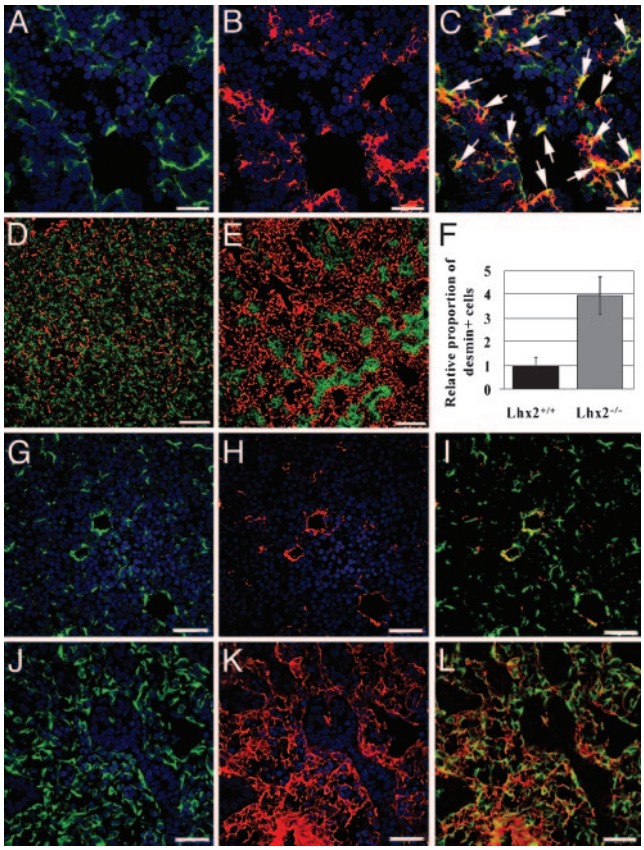

Fig. 2. Lhx2 is expressed in HSCs in fetal liver, and *Lhx2*$^{-/-}$ livers show increased proportion of HSCs with an activated phenotype. Histological sections of WT (*A–D* and *G–I*) and *Lhx2*$^{-/-}$ (*E* and *J–L*) livers. Confocal microscopy of an E13.5 WT liver section hybridized to an Lhx2 antisense probe (*B*, red) and subsequently immunostained with an anti-desmin antibody (*A*, green) show coexpression of desmin and Lhx2 in numerous cells indicated by yellow in the merged image (*C*, arrows). (*D* and *E*) Sections of E14.5 WT and mutant livers immunostained with anti-desmin (red) and anti-E-cadherin (green) antibodies to visualize stellate cells and endodermal cells, respectively. (*F*) Comparison of relative proportion of desmin-positive cells in WT and *Lhx2*$^{-/-}$ fetal livers. Confocal microscopy of E15.5 WT and mutant liver sections immunostained with an anti-desmin antibody (*G*, *J*, green) and an anti-ASMA antibody (*H* and *K*, red) show mainly coexpression of these genes in cells of the mutant liver in merged figures (*I* and *L*, yellow). (Scale bars indicate 30 μm in *A–C* and *G–L*, and 90 μm in *D* and *E*.)

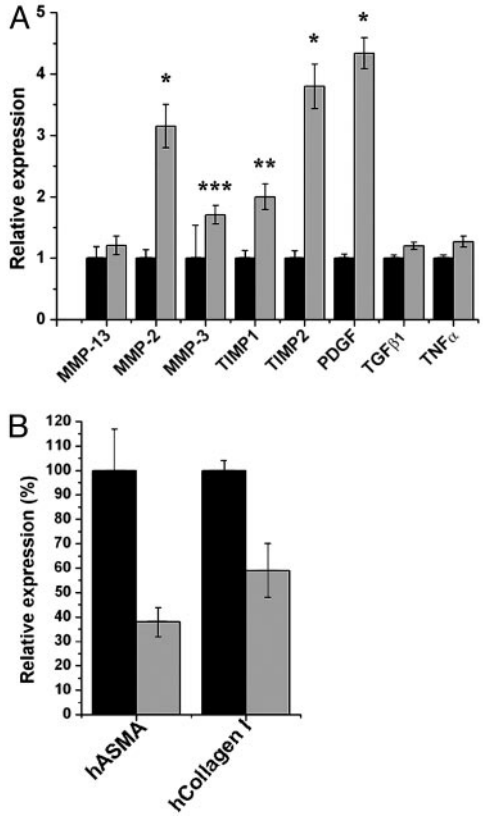

Fig. 3. Analysis of the relative expression levels of genes associated with activated HSCs. (*A*) Comparison between WT and mutant livers. Real-time PCR analyses were carried out on cDNA derived from E14.5 WT (black bars) and *Lhx2*$^{-/-}$ (gray bars) livers. The data are presented as the mean value from a representative experiment done in triplicates. *, $P < 0.0001$; **, $P < 0.001$; and ***, $P = 0.03$. Two additional analyses on independent cDNA preparations showed similar results. PDGF, platelet-derived growth factor; TGFβ1, transforming growth factor type β1; TNFα, tumor necrosis factor α. (*B*) Comparison between the human HSC line LX-2 transfected with either Lhx2 cDNA (gray bars) or vector control (black bars). The data are presented as mean value of a representative experiment done in triplicates. $P < 0.005$ for human ASMA (hASMA), and $P < 0.01$ for human collagen I (hCollagen I). Error bars indicate standard deviation.

observed in the WT livers at this stage (Fig. 4*N*), endothelial cells in the *Lhx2* mutant livers were often clustered and separated from the endodermal cells, and they often formed abundant vessel-like structures with dilated lumen (Fig. 4*O*), indicating an aberrant organization of the sinusoidal network. Thus, both the intrahepatic endoderm as well as the endothelium in the mutant liver displayed a distorted organization and the increase in ECM protein deposition appeared to precede the aberrant organization.

The Endodermal Cells in *Lhx2*$^{-/-}$ Fetal Livers Display an Altered Gene Expression Pattern. The ductular structures formed by the endodermal cells in the *Lhx2*$^{-/-}$ fetal liver resemble similar structures that are observed frequently during the regeneration process of cirrhotic livers, in livers displaying massive necrosis, and in certain animal models for liver regeneration and liver carcinogenesis (28–32). Reportedly, these ductular structures contain cells expressing both hepatoblast/hepatocyte-specific and bile-duct cell (cholangiocyte)-specific genes, and therefore, may represent a cellular response to the injury/insult that is mediated by a bipotent hepatic progenitor cell termed "oval cell." To compare the ductular structures in the mutant fetal livers to those in regenerating adult livers, we analyzed the gene expression profile of the hepatoblasts in the mutant livers. Early hepatoblasts express *AFP*, *albumin*, and low levels of *E-cadherin* (33, 34), whereas early cells committed to the biliary lineage express high levels of *E-cadherin* (35) and bile-duct-specific cytokeratins (34, 36). Analyses of mutant livers at E14.5 showed that the hepatoblasts in the mutant liver expressed high levels of all four genes (Fig. 5 *B*, *D*, *F*, and *H*). In contrast, few hepatoblasts were labeled with the bile-duct-specific anti-cytokeratin antibody in WT livers (Fig. 5*G*) and these cells expressed lower levels of *E-cadherin* (Fig. 5*C*) while maintaining expression of *AFP* and *albumin* (Fig. 5 *A* and *E*). The increased expression of bile-duct-cell-specific cytokeratin in the mutant liver was observed also at E13.5 but not before this stage (data not shown). The ductular structures appear to be enriched in cells expressing bile-duct-specific cytokeratin and high levels of *E-cadherin* in addition to the hepatoblast/hepatocyte-specific genes *AFP* and *albumin*. Thus, the endodermal cells in the mutant livers resemble the ductular structures observed during the regeneration process in a damaged adult liver also at the level of gene expression pattern.

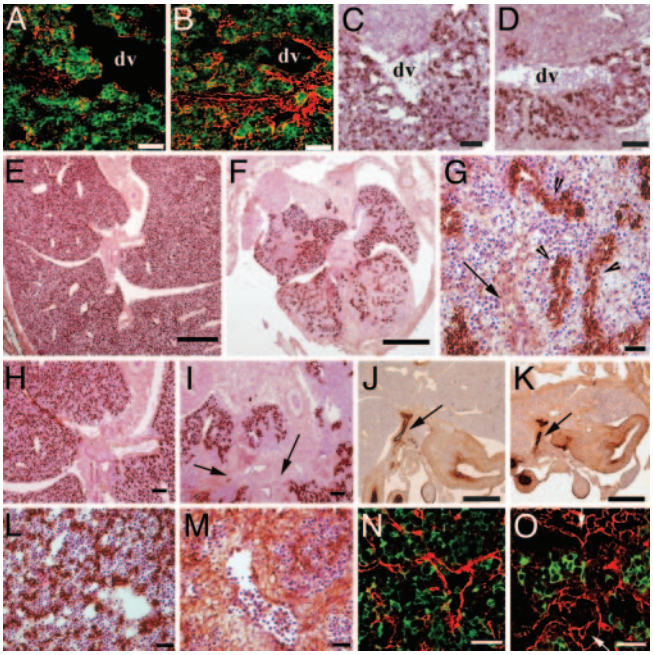

Fig. 4. Increased deposition of ECM proteins precedes a disrupted organization of the *Lhx2*$^{-/-}$ liver. Transversal sections of E11.5 WT (*A* and *C*) and mutant (*B* and *D*) livers were immunostained with an anti-E-cadherin antibody (green) to reveal hepatoblasts and an anti-collagen IV antibody (red) (*A* and *B*), or they were immunostained with the hepatoblast/hepatocyte-specific anti-albumin antibody (brown) and subsequently counterstained with hematoxylin–eosin (*C* and *D*). Transversal sections of E14.5 WT (*E*, *H*, *J*, *L*, and *N*) and mutant (*F*, *G*, *I*, *K*, *M*, and *O*) livers. Sections were immunostained with the hepatoblast/hepatocyte-specific anti-albumin antibody (brown) and subsequently counterstained with hematoxylin–eosin (*E–I*, *L*, and *M*), or stained with extrahepatic bile-duct-specific *D. biflorus* agglutinin (*J* and *K*, dark brown), or immunostained with the vascular endothelial-specific anti-PECAM antibody (red) and the hepatoblast-specific anti-AFP antibody (green) (*N* and *O*). Albumin-positive endodermal cells are distributed evenly throughout the liver lobes in the WT liver (*E*, *H*, and *L*), whereas the endodermal cells in mutant livers are unevenly distributed (*F* and *I*) and form ductular structures (*G*, arrow heads). Fibrous tissue is present in the hilum region of the *Lhx2*$^{-/-}$ liver (*I*, arrows), around blood vessels (*M*), and as fibrous septa throughout the liver (*G*, arrow). The extrahepatic biliary epithelium appears to be normal in mutant (*K*, arrow) embryos as compared with WT (*J*, arrow) embryos. A normal sinusoidal network is formed in the WT liver (*N*), whereas vessel-like structures with dilated lumen (arrows) are seen in the mutant liver (*O*). dv, ductus venosus. (Scale bars indicate 30 μm in *A*, *B*, *G*, and *L–O*; 100 μm in *C*, *D*, *H*, and *I*; and 500 μm in *E*, *F*, *J*, and *K*.)

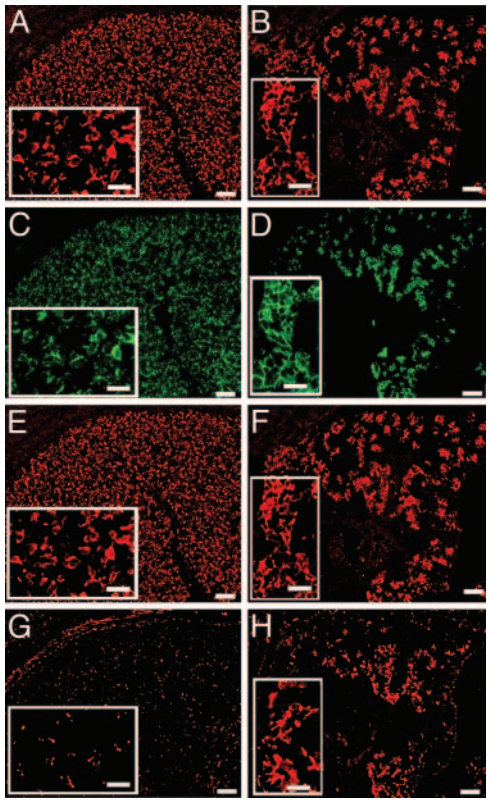

Fig. 5. The endodermal cells forming ductular structures in mutant livers are enriched in cells expressing both hepatoblast/hepatocyte-specific and cholangiocyte-specific genes. Consecutive transversal sections of an E14.5 WT (*A*, *C*, *E*, and *G*) and a mutant (*B*, *D*, *F*, and *H*) liver immunostained with an anti-albumin antibody (*A* and *B*, red), an anti-E-cadherin antibody (*C* and *D*, green), an anti-AFP antibody (*E* and *F*, red), or an anti-bile-duct-cell-specific cytokeratin antibody (*G* and *H*, red). Clusters of endodermal cells in the *Lhx2*$^{-/-}$ liver strongly express all four markers (*B*, *D*, *F*, and *H*), whereas the endodermal cells in the WT liver express lower levels of E-cadherin (*C*) and few WT endodermal cells express the bile-duct-cell-specific cytokeratin (*G*). (Scale bars indicate 100 μm in the main images and 30 μm in *Insets*.)

Discussion

We have shown that loss of Lhx2 expression in HSCs during embryonic development causes a progressive and spontaneous hepatic fibrosis. The mutant livers contain an increased proportion of mesenchymal cells expressing desmin, many of which also coexpress ASMA and, thus, resemble the activated HSCs described in the pathological process in hepatic fibrosis (11). *Lhx2*$^{-/-}$ livers display an increased expression level and accumulation of the ECM proteins implicated in adult liver fibrosis, including collagen types I, III, and IV, as well as laminin and fibronectin (10). Moreover, in agreement with previously reported data, the genes contributing to HSC activation, aberrant ECM remodeling, excessive ECM deposition, and collagen stabilization (such as platelet-derived growth factor, MMP-2 (gelatinase A), MMP-3 (stromelysin-1), TIMP1, TIMP2, and prolyl-4-hydroxylase) are up-regulated in the *Lhx2*$^{-/-}$ livers. During the fibrogenic process in adult liver, an ECM rich in interstitial collagens progressively replaces the normal perisinusoidal ECM. This shift in composition and amount of ECM perturbs the cellular organization of the liver, and this process is also observed in the developing liver of *Lhx2*$^{-/-}$ embryos. Collectively, our data suggest that Lhx2 is an important negative regulator of HSC activation and fibrogenesis, implying that loss of *Lhx2* expression in developing HSCs mimics the HSC activation process that is observed in adult fibrosis in both human and animal models for hepatic fibrosis. The down-regulated expression of genes associated with activated HSCs in the human HSC line LX-2 after transfection of Lhx2 cDNA supports this idea.

The duct-like appearance, together with the gene expression pattern of the endodermal cells in mutant fetal livers, reveals striking resemblance to the endodermal structures observed during the regenerative response in a damaged adult liver. Because these structures in adult liver are composed of cells expressing hepatoblast/hepatocyte-specific as well as cholangiocyte-specific genes, they have been suggested to represent a regenerative response mediated by oval cells (28–32). Animal models for liver regeneration have shown that activated HSCs are associated closely with these ductular structures (31) and most likely play a role in the regenerative response in adult liver (37). The dramatic increase in activated HSCs in the *Lhx2*$^{-/-}$ livers suggests that these cells play a role in the formation and/or maintenance of similar structures that are also in fetal liver. Similar to oval cells, early hepatoblasts in fetal liver are bipotent

and can generate both hepatocytes and cholangiocytes (38, 39). Therefore, the lack of Lhx2 in HSCs appears to provide signals to the early hepatoblasts in fetal liver that promote a regenerative response similar to that in adult liver. Although the role of Lhx2 in HSCs during the regenerative response in adult liver remains to be elucidated, our data imply that Lhx2 expression in developing HSCs is important for proper liver morphogenesis during embryonic development. Moreover, the $Lhx2^{-/-}$ phenotype could, in principle, be considered as a congenital syndrome. However, the fibrogenic process, together with the organization of the endoderm, is more comparable with the wound-healing response in adult liver. This observation does not exclude that a certain subgroup(s) of congenital hepatic fibrosis might be caused by mutations in Lhx2 or an Lhx2-associated pathway(s), because congenital hepatic fibrosis is a group of genetically distinct disorders (3).

Elucidation of the molecular mechanisms mediating the activation of HSCs is important for understanding the fibrogenic process. However, most studies have focused on genes that are up-regulated upon HSC activation (40–43). Our finding might represent a paradigm shift in the search for genes mediating activation of HSCs, because it implies that down-regulation of Lhx2 in HSCs leads to activation. We have previously shown that Lhx2 is expressed in HSCs in adult mice (14), suggesting that inactivation of Lhx2 in adult liver results in a similar phenotype. Although a putative function of Lhx2 in human HSCs remains to be elucidated, the down-regulation of fibrosis-associated genes in a human HSC line transfected with Lhx2 cDNA suggests that Lhx2 negatively regulates the fibrogenic process also in humans. Elucidation of the molecular mechanisms by which lack of Lhx2 expression activates HSCs and, thus, promotes fibrogenesis could provide insights and clues to treatment and prevention of hepatic fibrosis. In conclusion, the lack of Lhx2 in developing HSCs provokes a series of pathological events sharing many characteristics with the wound-healing response in adult liver. Thus, the $Lhx2^{-/-}$ mouse embryos could provide a reproducible model system to study the early pathological events leading to hepatic fibrosis.

We thank Dr. Thomas Edlund for critical reading of this manuscript and Nary Veal, Carlos Alvarez, and Steven Yea for technical assistance. This work was supported by the Swedish Cancer Society, a grant from the Västerbotten county, the Umeå University Biotechnology Fund, National Institutes of Health Grant DK56621 (to S.L.F.), and the Feld Fibrosis Research Fund (to S.L.F.). L.C. is supported by the Tobias Foundation and by a grant from the European Union Regional Fund (Objective 1).

1. Friedman, S. L. (2000) *J. Biol. Chem.* **275,** 2247–2250.
2. Hui, A. Y. & Friedman, S. L. (2003) *Expert. Rev. Mol. Med.* **2003,** 1–23.
3. Desmet, V. J. (1992) *Histopathology* **20,** 465–477.
4. Iredale, J. P. (2003) *Br. Med. J.* **327,** 143–147.
5. Hahn, E., Wick, G., Pencev, D. & Timpl, R. (1980) *Gut* **21,** 63–71.
6. Rojkind, M., Giambrone, M. A. & Biempica, L. (1979) *Gastroenterology* **76,** 710–719.
7. Kmiec, Z. (2001) *Adv. Anat. Embryol. Cell Biol.* **161,** III–XIII, 1–151.
8. Ramadori, G. (1991) *Virchows Arch. B Cell Pathol.* **61,** 147–158.
9. Enzan, H., Himeno, H., Hiroi, M., Kiyoku, H., Saibara, T. & Onishi, S. (1997) *Microsc. Res. Tech.* **39,** 336–349.
10. Bedossa, P. & Paradis, V. (2003) *J. Pathol.* **200,** 504–515.
11. Bissell, D. M. (1992) *Gastroenterology* **102,** 1803–1805.
12. Gressner, A. M. & Bachem, M. G. (1995) *Digestion* **56,** 335–346.
13. Friedman, S. L., Roll, F. J., Boyles, J. & Bissell, D. M. (1985) *Proc. Natl. Acad. Sci. USA* **82,** 8681–8685.
14. Kolterud, A., Wandzioch, E. & Carlsson, L. (2004) *Gene. Expr. Patterns* **4,** 521–528.
15. Porter, F. D., Drago, J., Xu, Y., Cheema, S. S., Wassif, C., Huang, S. P., Lee, E., Grinberg, A., Massalas, J. S., Bodine, D., Alt, F. & Westphal, H. (1997) *Development (Cambridge, U.K.)* **124,** 2935–2944.
16. Maher, J. J. & McGuire, R. F. (1990) *J. Clin. Invest.* **86,** 1641–1648.
17. Monuki, E. S., Porter, F. D. & Walsh, C. A. (2001) *Neuron* **32,** 591–604.
18. Harlow, E. & Lane, D. (1999) *Using Antibodies: A Laboratory Manual* (Cold Spring Harbor Lab. Press, Plainview, NY).
19. Herbst, H., Frey, A., Heinrichs, O., Milani, S., Bechstein, W. O., Neuhaus, P. & Schuppan, D. (1997) *Histochem. Cell Biol.* **107,** 399–409.
20. Yokoi, Y., Namihisa, T., Kuroda, H., Komatsu, I., Miyazaki, A., Watanabe, S. & Usui, K. (1984) *Hepatology* **4,** 709–714.
21. Ballardini, G., Fallani, M., Biagini, G., Bianchi, F. B. & Pisi, E. (1988) *Virchows Arch. B Cell Pathol.* **56,** 45–49.
22. Ramadori, G., Veit, T., Schwogler, S., Dienes, H. P., Knittel, T., Rieder, H. & Meyer zum Buschenfelde, K. H. (1990) *Virchows Arch. B. Cell Pathol.* **59,** 349–357.
23. Arthur, M. J. (2000) *Am. J. Physiol.* **79,** G245–G249.
24. Benyon, R. C. & Arthur, M. J. (2001) *Semin. Liver Dis.* **21,** 373–384.
25. Iredale, J. P., Benyon, R. C., Pickering, J., McCullen, M., Northrop, M., Pawley, S., Hovell, C. & Arthur, M. J. (1998) *J. Clin. Invest.* **102,** 538–549.
26. Pinzani, M. & Marra, F. (2001) *Semin. Liver Dis.* **21,** 397–416.
27. Xu, L., Hui, A., Albanis, E., Arthur, M., Mukherjee, P., Friedman, S. & Eng, F. (2004) *Gut*, in press.
28. Vandersteenhoven, A. M., Burchette, J. & Michalopoulos, G. (1990) *Arch. Pathol. Lab. Med.* **114,** 403–406.
29. Rubin, E. M., Martin, A. A., Thung, S. N. & Gerber, M. A. (1995) *Am. J. Pathol.* **147,** 397–404.
30. Thorgeirsson, S. S. (1996) *FASEB J.* **10,** 1249–1256.
31. Paku, S., Schnur, J., Nagy, P. & Thorgeirsson, S. S. (2001) *Am. J. Pathol.* **158,** 1313–1323.
32. Sell, S. (2002) *Semin. Cell. Dev. Biol.* **13,** 419–424.
33. Shiojiri, N. (1997) *Microsc. Res. Tech.* **39,** 328–335.
34. Shiojiri, N. (1994) *Cell Tissue Res.* **278,** 117–123.
35. Terada, T., Ashida, K., Kitamura, Y., Matsunaga, Y., Takashima, K., Kato, M. & Ohta, T. (1998) *J. Hepatol.* **28,** 263–269.
36. Clotman, F., Lannoy, V. J., Reber, M., Cereghini, S., Cassiman, D., Jacquemin, P., Roskams, T., Rousseau, G. G. & Lemaigre, F. P. (2002) *Development (Cambridge, U.K.)* **129,** 1819–1828.
37. Mabuchi, A., Mullaney, I., Sheard, P. W., Hessian, P. A., Mallard, B. L., Tawadrous, M. N., Zimmermann, A., Senoo, H. & Wheatley, A. M. (2004) *J. Hepatol.* **40,** 910–916.
38. Rogler, L. E. (1997) *Am. J. Pathol.* **150,** 591–602.
39. Lowes, K. N., Croager, E. J., Olynyk, J. K., Abraham, L. J. & Yeoh, G. C. (2003) *J. Gastroenterol. Hepatol.* **18,** 4–12.
40. Hellerbrand, Wang, S. C., Tsukamoto, H., Brenner, D. A. & Rippe, R. A. (1996) *Hepatology* **24,** 670–676.
41. Lalazar, A., Wong, L., Yamasaki, G. & Friedman, S. L. (1997) *Gene* **195,** 235–243.
42. Ikeda, K., Kawada, N., Wang, Y. Q., Kadoya, H., Nakatani, K., Sato, M. & Kaneda, K. (1998) *Am. J. Pathol.* **153,** 1695–1700.
43. Ratziu, V., Lalazar, A., Wong, L., Dang, Q., Collins, C., Shaulian, E., Jensen, S. & Friedman, S. L. (1998) *Proc. Natl. Acad. Sci. USA* **95,** 9500–9505.